Third International Conference on Sustainable Construction Materials and Technologies http://www.claisse.info/Proceedings.htm

Crack spacing in steel bar reinforced strain hardening cement-based composites (R/SHCC), towards corrosion modelling

G.P.A.G. van Zijl and S.C. Paul

Department of Civil Engineering, Stellenbosch University
Private Bag X1, Matieland, 7602, South Africa
gvanzijl@sun.ac.za, suvashpl@sun.ac.za

ABSTRACT

Durability of strain-hardening cement-based composites (SHCC) is studied, with particular reference to corrosion resistance it may offer embedded steel reinforcement (R/SHCC) through inherently controlled crack width and spacing. Recent research results show that cracks act as pathways for fast ingress of chloride and water to the steel bar surface, but that the corrosion rates in cracked R/SHCC are low relative to RC or R/mortar. An accompanying paper (Paul et al. 2013a) presents the test program and results of accelerated chloride-induced corrosion of pre-cracked R/SHCC specimens with three levels of cover depths and two levels of steel bar reinforcement. Here, the flexural crack width distributions and spacing in R/SHCC are presented, indicating insensitivity to cover depth and steel bar reinforcement level in the given cover and reinforcement ranges, supporting a modeling approach of crack width and spacing limitation to limit electro-chemical corrosion cell size.

Keywords. SHCC, Corrosion, Chloride, Crack distribution, Crack spacing

INTRODUCTION

The state-of-the-art of durability of strain hardening cement-based composites (SHCC) (van Zijl & Wittmann, 2011, van Zijl et al. 2012) reports on the multiple cracking characteristic of this relatively young construction material and the reduced ingress rates of substances associated with deterioration of cement-based composites. See Figure 1 as a demonstration of the controlled, fine cracking in SHCC under uniaxial tension. Chloride-induced corrosion in R/SHCC (steel bar reinforced SHCC), as expected in regions along coasts or of de-icing by salt spraying practice, was identified as an significant deterioration method in terms of global infrastructure repair expenditure.

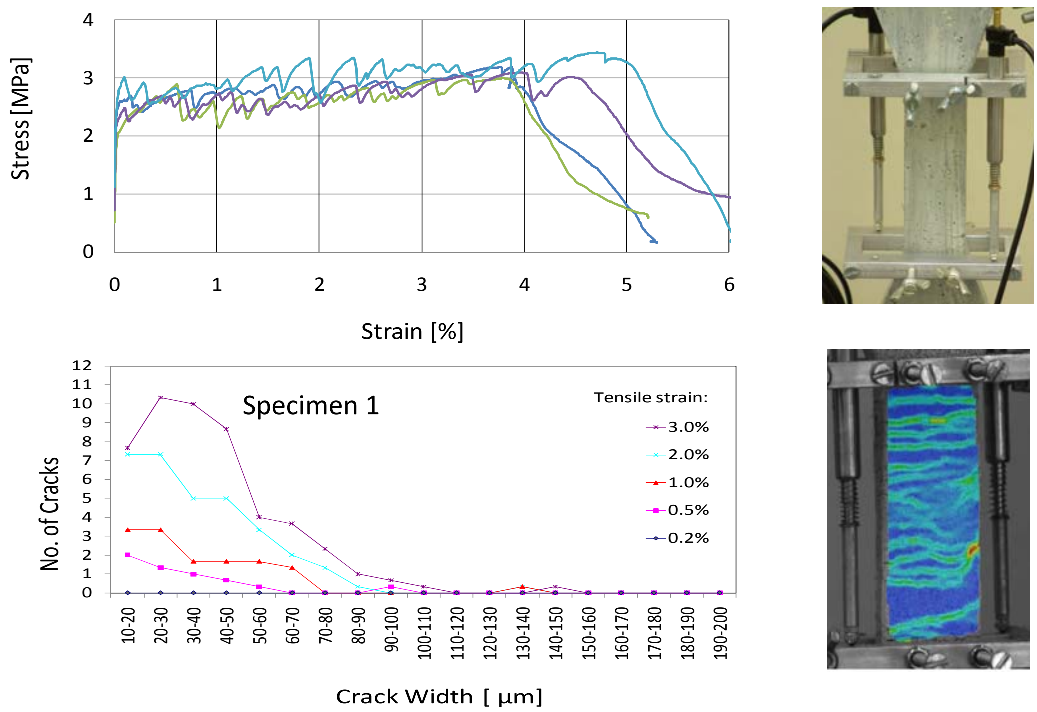

Figure 1. Crack width distributions in SHCC under uniaxial tension

Chloride, water and oxygen ingress in SHCC

The corrosion resistance durability potential of SHCC, believed to be due to the fine, controlled crack widths, was demonstrated by results of dominant micro-cell corrosion in finely cracked R/SHCC versus dominant macro-cell corrosion in cracked R/mortar by Miyazato & Hiraishi (2005). Recent research results indicate that, whilst effective chloride diffusion coefficients are lower in cracked R/SHCC than in R/mortar beams (Sahmaran et al. 2007), cracks act as pathways for fast ingress deep into mortar (Wittmann et al. 2011, Altmann 2012, Paul et al. 2013a). Chloride penetrated to a height of 65 mm in 1 hour, and up to 84 mm in 3 hours in cracked SHCC (Paul et al. 2013a). The increased ingress rates of oxygen and water into SHCC once cracked, were summarised recently by van Zijl (2011).

Crack width vs crack spacing as dominant corrosion mechanism

Recent accelerated chloride-induced corrosion experimental results of R/mortar and R/HFRCC (hybrid fibre reinforced cement-based composites) beams, pre-cracked in flexure to various maximum crack widths (0.12 - 0.36 mm in R/mortar, 0.12 - 0.51 mm in R/HFRCC), were reported to indicate a correlation between the initial crack width and the corrosion rate, steel mass loss, and residual rebar tensile strength (Mihashi et al. 2011a). Unfortunately the crack width distribution, number of cracks and crack spacing were not reported. Ahmed et al. (2010) reported steel mass loss of 0.5 g in R/HFRCC as opposed to 16.6 g in R/mortar after 92 days of accelerated chloride-induced corrosion of beams of cross section 100 mm x 100 mm with one 10 mm diameter steel bar and 20 mm cover. Photographic evidence indicated an average crack spacing of about 20 mm, i.e. 10 cracks, 7 of width 0.02 mm, 2 of 0.03 mm and one of 0.06 mm, spread over in a length of 200 mm, but a single 0.16 mm wide crack in R/mortar. The roles of crack width and spacing cannot be distinguished from these results.

Accelerated chloride-induced corrosion tests on larger scale uncracked and pre-cracked beams (300 mm deep, 210 mm wide, 2500 mm long, containing 3 lower (tensile) bars of 16 mm diameter, and 6 mm diameter stirrups at 80 mm minimum spacing with 45 mm clear cover) were recently performed by Maalej et al. (2007). They compared RC beams with functionally graded (FGC) beams containing DFRCC (ductile fibre-reinforced cementitious composites, exhibiting multiple cracks in flexure) in the tensile zone encapsulating the tensile reinforcing bars, and ordinary concrete in the remainder of the beam section. After 93 days of cyclic wetting and drying chloride exposure of the pre-cracked beams, and even up to 143 days in the case of one pre-cracked FGC beam, insignificant corrosion was observed after physical removal of the cover layer, while extensive corrosion was clear on the RC beams. Unfortunately, the pre-crack patterns (nr of cracks, crack spacing) were not reported, except the maximum crack widths of 0.54 mm under load (reduced to 019 mm after unloading), 0.28 mm (0.12 mm) and 0.3 mm (0.13 mm) in the RC and two R/DFRCC beams respectively. Note that the chloride exposure was performed in the unloaded state.

Corrosion-induced cracking and spalling

In their accelerated chloride-induced corrosion experiments on uncracked R/mortar and R/HFRCC, Mihashi et al. (2011b) reported the initiation of an expansive corrosion crack parallel to the steel bar in the R/mortar specimens after 27 weeks, which grew rapidly to a significant width, but no such crack arose in the R/HFRCC beams during the 52 duration of the accelerated corrosion testing. Such longitudinal cracks arose after 30 days of accelerated testing of larger pre-cracked RC beams by Maalej et al. (2007), but none in their pre-cracked R/DFRCC beams. This may be attributed to either or both the reduced corrosion rate or / and fibre crack bridging. Steel mass loss was calculated from Faraday's law:

$$\Delta m = \frac{MIt}{ZF} \qquad (1)$$

with M the atomic mass of iron (56 g/mole), I the corrosion current (A), t the time (s), Z the valency of iron (2) and F the Faraday constant (96 500 A s). After the test period of 1 year, the actual mass loss was determined by a gravimetric method – see Figure 2a.

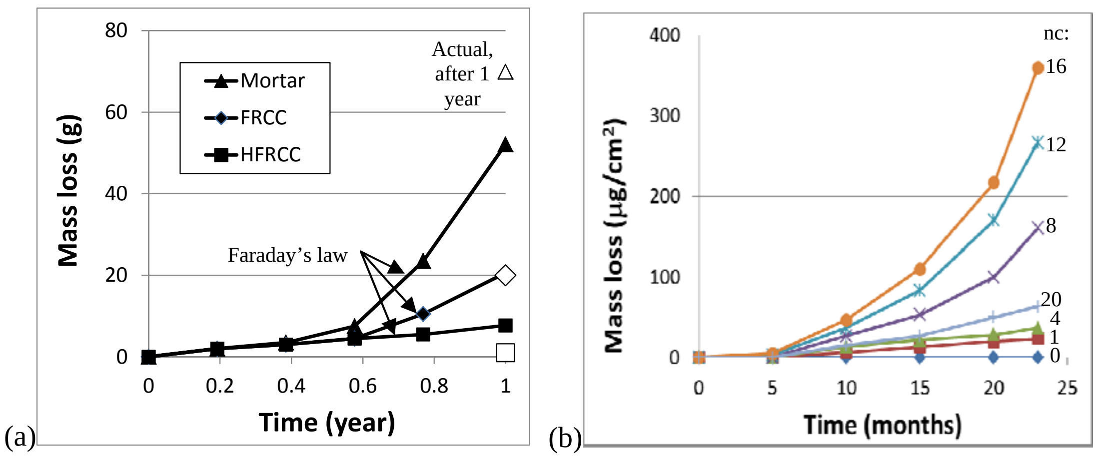

Figure 2. Steel mass loss in (a) non pre-cracked R/mortar, R/FRCC and R/HFRCC, reproduced from Mihashi et al. (2011), (b) RC with different numbers of cracks (reproduced from Arya & Ofori-Darko 1996).

TOWARDS MODELLING CORROSION IN R/SHCC

Prediction models for chloride-induced corrosion generally assume uncracked concrete, while design standards generally limit crack widths. Cracks act as pathways for ingress of chlorides, which de-passivate the protective local environment of steel in concrete, causing dissolution of iron into the pore water. Ingress of water and oxygen either in the wide crack, or through the cover concrete, forms the cathode of the chemo-electrical corrosion cell by formation of hydroxyls in close vicinity of the anode in the crack zone (micro-cell) or at passive steel further away in uncracked regions (macro-cell).

A vast pool of research data on RC corrosion has been developed over the past several decades, including the reduced density, or increased volume of various corrosion products (FeO, Fe_3O_4, $Fe(OH)_3$ $3H_2O$, etc.; Liu & Weyers 1998), the time to corrosion cracking due to pressure build-up once the porous interfacial zone surrounding the steel is exceeded, but also about the role of crack width and spacing. It is generally agreed that the probability of corrosion is increased with increased crack width. This is strengthened by the results of Arya & Ofori-Darko (1996) shown in Figure 2b, considering that the specimens used to produce the shown results had varying numbers of artificially formed cracks (0, 1, 2, 4, 8, 12 and 20), but of equal total width (2.5 mm) over the same length of about 1300 mm. this means that the crack width and spacing varied from w_c = 0.125 mm and s_c = 67 mm in the case of 20 cracks, to a single crack with w_c = 2.5 mm. The significant change in corrosion rate trend from the fast corroding specimens containing 16 cracks (w_c = 0.156 mm, s_c = 84 mm) to the low corroding rate in specimens with 20 cracks seen in Figure 2b, is believed to indicate the importance of crack spacing, and the coinciding corrosion cell size. This motivates the investigation of crack width and spacing in R/SHCC in the next sections.

SPECIMEN PREPARATION

The same SHCC mix as reported in an accompanying paper in this Proceedings (Paul et al. 2013a) was used, containing 390 kg of CEM I 52.5, 670 kg of class F fly ash, 390 L of water, 550 kg of sand and 26 kg of Poly-vinyl Alcohol fibres per cubic meter of SHCC. The fibres are of length 12 mm and diameter 40 μm. One set of specimens, denoted FS-R/SHCC, was prepared with the more usual fine sand, available locally in South Africa as Console type 2 foundry sand with maximum particle 0.3 mm. A complete, separate set of specimens, denoted CS-R/SHCC) was prepared with a local sand with maximum particle size 1.8 mm. More details of these mixes, and their strain-hardening uniaxial tensile responses are given in Paul et al. (2013a).

From these SHCC mixes, small SHCC beam specimens of 100 mm x 100 mm x 500 mm were prepared, reinforced with either one bar (reinforcement level ρ_s = 0.8% of nominal cross-section) or two steel bars (ρ_s = 1.6%) of 10 mm diameter and characteristic yield strength of 450 MPa and E-modulus 206 GPa. For both reinforcement levels, cover depths of 15 mm, 25 mm and 35 mm were prepared. Three beams per specimen type were prepared, giving in total 36 specimens (3 per set, 3 cover depths, 2 levels of reinforcement, 2 sand types). The beams were cast and vibrated in steel moulds, protected under laboratory conditions until stripping after 48 hours, placed in curing tanks at 23 ± 2 ^{o}C for 7 days and then placed in a controlled environment at 23 ± 2 ^{o}C and 60 ± 5 % relative humidity until the age of 28-30 days before commencing with flexural testing.

The beams were subjected to three point bending to a central deflection level of 3.5 mm to study the crack pattern, and subsequently chloride-induced corrosion exposure. Note that the crack width measurements and corrosion testing were performed in the unloaded state. The flexural test setup and responses are shown in Figure 3. After unloading, the crack patterns were studied, as discussed in the section below, before the specimens were sealed for specific chloride exposure – see Figure 3 for sealing details. A solvent free epoxy protective coating (Sikaguard 63N) was used.

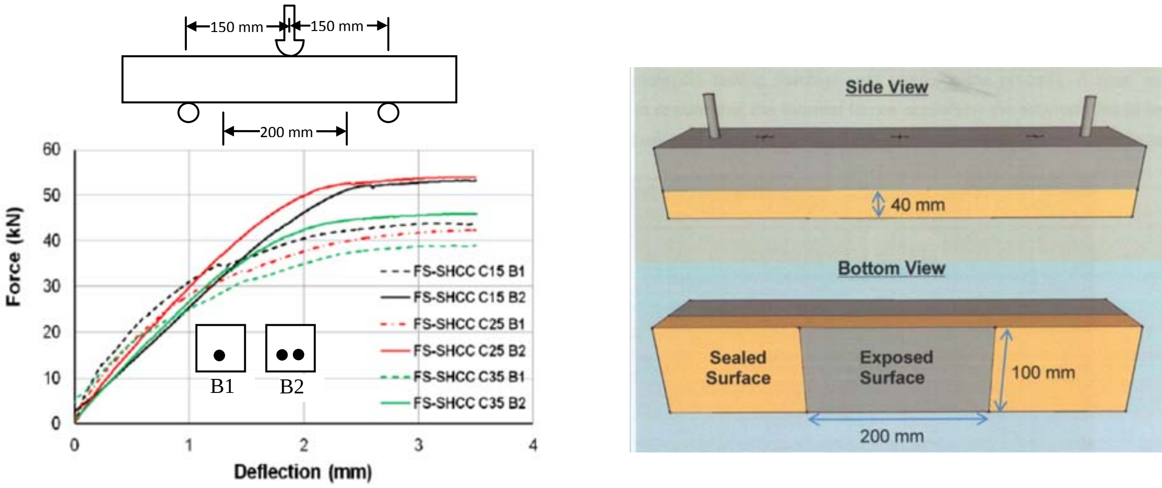

Figure 3. R/SHCC beam pre-cracking and sealing for selective exposure

EXPERIMENTAL RESULTS

The influence of steel bar reinforcement and cover depth on crack width and spacing in R/SHCC is reported here. This is considered to be essential information for understanding, characterising and prediction corrosion in R/SHCC.

Cracking definition and measurement

After unloading the central load in three point bending, the central 200 mm length of each beam was observed carefully for cracks, with the aid of a Leica M27.5 microscope. Crack widths and spacing were measured on the far tensile face only. Three lines were drawn parallel to the steel bar(s) on the tensile face over the central 200mm. These lines were spaced equally, i.e. 25 mm apart. Transverse cracks passing through at least two of the three lines were considered. Crack widths were determined by comparison with a line width template, containing crack widths in 50 μm intervals, i.e. 50 μm, 100 μm, etc. In this way, cracks were categorised in the intervals $0 < w_c \leq 50$ μm, $50 < w_c \leq 100$ μm, etc.

Cracking width and spacing

The results are summarised in Table 1 and shown in the form of crack width histograms in Figure 4. In Figure 5, the influence of cover depth on average crack spacing is illustrated. It must be kept in mind that the crack spacing is for fully developed crack patterns, after flexural loading to ultimate resistance in order to create a well-developed crack pattern for subsequent corrosion testing. From the Figure 5, the crack spacing appears to be either reduced with increased cover depth (Figure 5a for FS-R/SHCC), or insensitive to cover depth.

This is the opposite effect of that in RC, where an increased crack width is usually associated with increased cover depth, as provided for instance in Eurocode 2 (BS EN1992-1-1:2004). Note that the specimens containing two steel bars exhibited several diagonal cracks at the beam ends in the region of the supports outside the central 200 mm exposure length, indicating shear dominance at this level of flexural reinforcement. These cracks fell outside the central 200 mm, and were sealed as shown in Figure 3b.

Table 1. Crack distribution in R/SHCC containing 1 reinforcing bar (B1)

1 Bar specimens		Fine sand			Coarse sand		
Cover (mm)	Specimen	Nr of cracks		Avg. spacing (mm)	Nr of cracks		Avg. spacing (mm)
		$0 < w_c \leq 50$ µm	$w_c >$ 50 µm		$0 < w_c \leq 50$ µm	$w_c >$ 50 µm	
15	1	18	1 (100)	10.5	17	3 (250)	10.0
	2	19	1 (200)	10.0	21	1 (100)	9.1
	3	20	1 (200)	9.5	16	2 (250)	11.1
	Avg	19.0	1.0	**10.0**	18.0	2.0	**10.0**
25	1	26	0 (50)	7.7	22	2 (200)	8.3
	2	16	2 (200)	11.1	12	2 (700)	14.3
	3	18	1 (150)	10.5	20	0 (50)	10.0
	Avg	20.0	1.0	**9.5**	18.0	1.3	**10.3**
35	1	21	4 (200)	8.0	15	2 (250)	11.8
	2	20	1 (100)	9.5	18	1 (400)	10.5
	3	20	3 (400)	8.7	18	1 (150)	10.5
	Avg	20.3	2.7	**9.7**	17.0	1.3	**10.9**

Table 2. Crack distribution in R/SHCC containing 2 reinforcing bars (B2)

2 Bar specimens		Fine sand			Coarse sand		
Cover (mm)	Specimen	Nr of cracks		Avg. spacing (mm)	Nr of cracks		Avg. spacing (mm)
		$0 < w_c \leq 50$ µm	$w_c >$ 50 µm		$0 < w_c \leq 50$ µm	$w_c >$ 50 µm	
15	1	9	2 (150)	19.2	16	1 (150)	11.8
	2	11	1 (100)	16.7	15	2 (100)	11.8
	3	9	2 (200)	18.2	15	1 (250)	12.5
	Avg	9.7	1.7	**17.6**	15.3	1.3	**12.0**
25	1	15	1 (100)	12.5	15	0 (50)	13.3
	2	14	0 (50)	14.3	12	2 (100)	14.3
	3	15	0 (50)	13.3	17	0 (50)	11.8
	Avg	14.7	0.3	**13.3**	14.7	0.7	**13.0**
35	1	15	0 (50)	13.3	14	2 (250)	12.5
	2	14	2 (100)	12.5	18	0 (50)	11.1
	3	15	2 (150)	11.8	17	1 (100)	11.1
	Avg	14.7	1.3	**12.5**	16.3	1.0	**11.5**

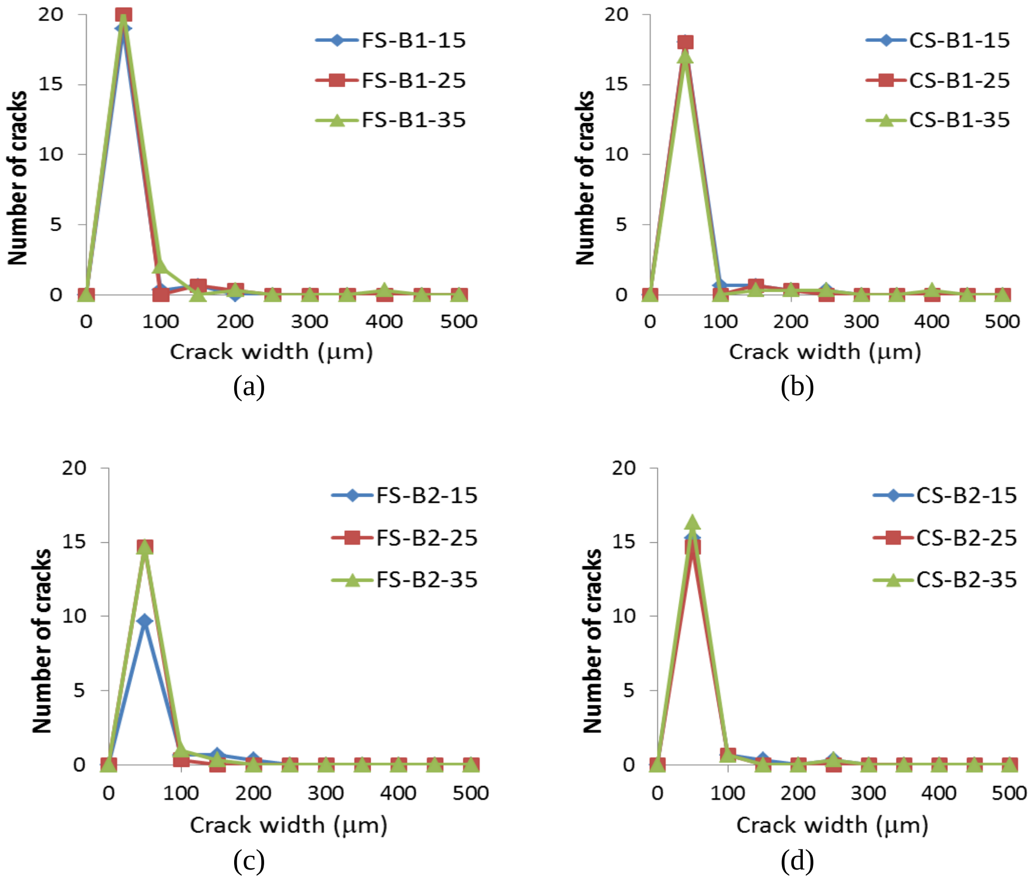

Figure 4. Crack width distributions in (a) FS-B1 (b) CS-B1 (c) FS-B2 (d) CS-B2

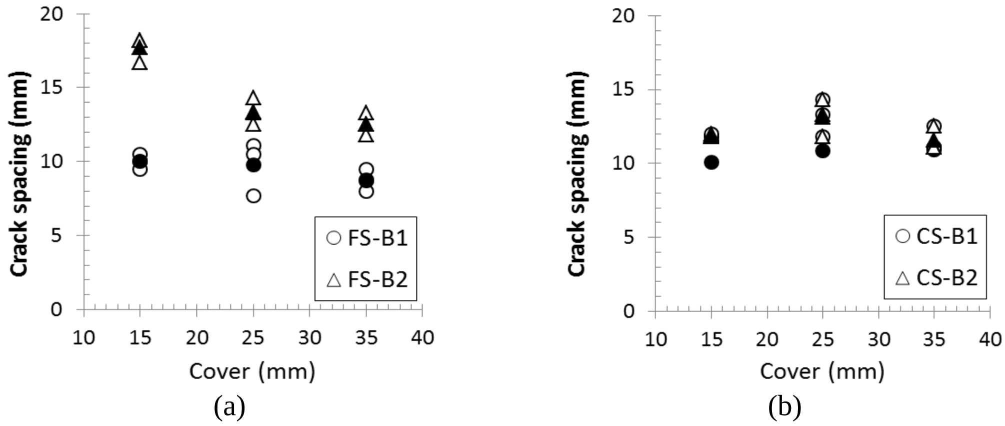

Figure 5. Crack spacing in (a) FS – R/SHCC and (b) CS – R/SHCC. Note that the average spacing for each cover depth is shown with a filled-in symbol.

FLEXURAL CRACK SPACING IN R/SHCC

It has been postulated that crack spacing in SHCC is not a structural property, but a material property, implying that crack spacing is independent of structural size (Li &

Stang 2004). Crack spacing in SHCC is determined by the fibre and matrix properties, as well as their interfacial interaction. The concept of crack saturation refers to the final number of cracks, which depends on the strain level, but also the margin between fibre pull-out complementary energy and matrix crack tip toughness (Kanda & Li 1998).

Figure 6 suggests that the reinforcing bar geometry may influence the crack spacing. It shows the crack patterns in RC and R/SHCC (R/ECC) as reported by Fischer & Li (2004). It appears that the cracks at the rebar interface in R/ECC coincide to a significant degree with the rebar pitch. In this case of uniaxial tension applied to the reinforcing bar, crack kinking, intersecting and branching in the cover leads to a different surface crack pattern. The steel bars used in the R/SHCC specimens reported in this paper have a similar geometrical form, with pitch of about 6mm. Recall the average crack spacing of about 10 mm (9.7 – 10.9 mm) for all specimens containing a single rebar in both FS-SHCC and CS-SHCC beams for all three cover depths. For the specimens containing two steel bars, the average crack spacing is roughly double the rebar pitch, except the FS specimens with 15 mm cover, where the spacing is as high as 18 mm, or three times the rebar pitch.

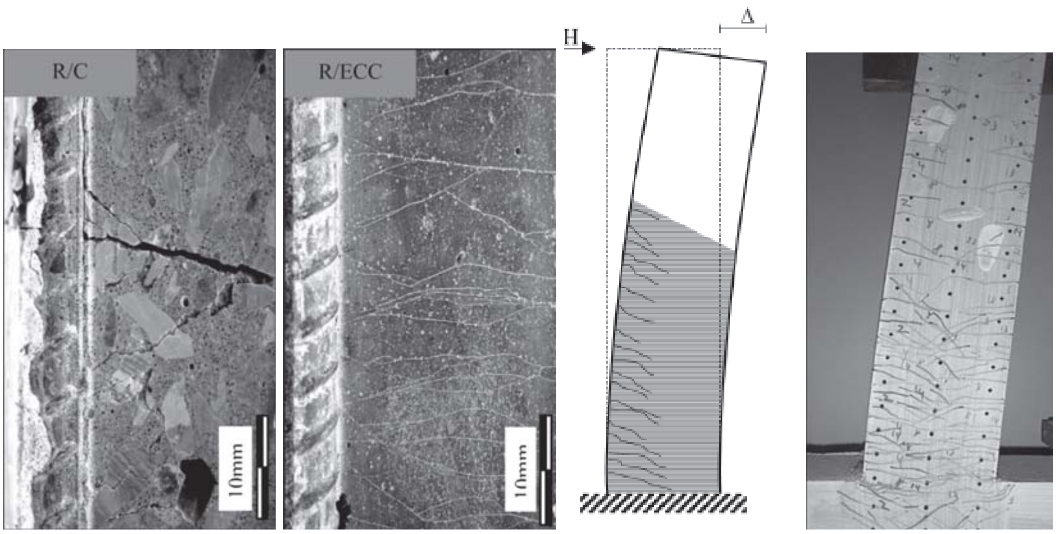

Figure 6. Uniaxial tensile crack patterns in (from left to right) RC, R/SHCC (R/ECC) specimens, and cyclic flexural cracks in an R/ECC element (Fischer & Li 2002).

CONCLUSIONS

Whilst cracks allow relatively fast ingress of chlorides, oxygen and water required for chloride-induced corrosion of steel embedded in SHCC, recent results reported by several research groups indicate low corrosion rates in pre-cracked R/SHCC. Motivated by experimental evidence of favourable, low corrosion rate in RC specimens containing several relatively fine and finely spaced cracks, crack width and crack spacing in R/SHCC were studied in an experimental program and reported here. The following conclusions can be drawn:

Flexural crack spacing in R/SHCC

- The average flexural crack spacing in R/SHCC containing a single reinforcing bar is insensitive to cover depths in the range 15 – 35 mm. In the tests reported here, the steel bar reinforcement level was 0.8% by volume. An average crack spacing of 9.7 – 10.9 mm was found for both FS-R/SHCC and CS-R/SHCC.

- For R/SHCC containing two steel bars, i.e. 1.6% by volume, the crack spacing was slightly higher at a roughly 12 mm. The exception was a higher average of 18 mm for a cover depth of 15 mm in FS-R/SHCC. The increased flexural crack spacing may be due to shear dominance at this high steel bar reinforcement.

Flexural crack width in R/SHCC

- The crack width distribution in R/SHCC containing a single reinforcing bar is insensitive to cover depths in the range 15 – 35 mm, considering a crack width interval of 50 μm. This was found for both FS-R/SHCC and CS-R/SHCC. In both specimen types, by far the most cracks (17-18 in CS, 19-20 in FS in the 200 mm observation length) were found to be 50 μm wide or less, and only a few (3-4 in CS, 2-3 in FS) of greater width.

- In R/SHCC containing two steel bars the crack with distribution is also insensitive to cover depths in the range 15 – 35 mm. FS specimens with 15 mm cover were the exception, containing 10 cracks of 50 μm or less, as opposed to 15 each in FS specimens with 25 and 35 mm cover. The CS specimens contained 15-16 cracks in this width category. 1-3 cracks in both CS and FS were wider than 50 μm.

The corrosion testing of these specimens are on-going, having been exposed for 52 days at the time of this report. As reported in the accompanying paper (Paul et al. 2013a), no active corrosion has been detected thus far, although slight discolouration was observed in densely cracked regions in three specimens which were selected to be broken open in order to study the steel bar corrosion.

Note that a high level of deformation was applied to all beams in this project. Crack width and spacing characterisation in R/SHCC, as well as the chloride induced corrosion of such specimens will be studied at service load levels in future work, to enable the development of design guidelines and modelling capacity of corrosion of R/SHCC.

REFERENCES

Ahmed SFU, Mihashi H 2010. Corrosion durability of strain hardening fibre-reinforced cementitious composites, Australian J Civil Engineering Online.

Alttmann, F. 2012. A durability concept for strain-hardening cement-based composites, PhD dissertation, Technical University of Dresden, 192 pp.

Arya C, Ofori-Darko FK 1996. Influence of crack frequency on reinforcement corrosion in concrete, Cement an dConcrete Research 26(3): 345-353.

Boshoff W.P. (2011). Performance based approach to modelling SHCC cracking for durability, FIB Workshop on Performance based specifications of concrete, Leipzig,

Germany, June 2011.
BS EN1992-1-1:2004. EUROCODE 2 Design of concrete structures - Part 1: General rules for buildings, BSI.
Fischer G, Li VC 2004. Effect of fiber reinforcement on the response of structural members, FramCoS 2004, pp 831-838.
Kanda T, Li VC 1998. Multiple cracking sequence and saturation in fibre reinforced cementitious composites.
Koichi Kobayashi, Takahiro Iizuka, Hoshito Kurachi, Keitetsu Rokugo. Corrosion protection of high performance fiber reinforced cement composites as a repair material, Cement and Concrete Research 32 (2010) 411-420.
Li VC, Stang H 2004. Elevating FRC material ductility to infrastructure durability, Proceedings BEFIB 2004, September, Varenna, pp. 171-186.
Liu Y, Weyers RE 1998. Modeling the time-to-corrosion cracking in chloride contaminated reinforced concrete structures, ACI Materials J 95(1): 675-681.
Mihashi H, Ahmed SFU, Kobayakawa A 2011a. Influence of crack width on corrosion of steel bar in fiber reinforced cementitious composites, in C Leung and KT Wan (ed), Int. RILEM Conference on Advances in Construction Materials Through Science and Engineering, Hong Kong, Sep 5-7 2011, pp. 602-609.
Mihashi H., Ahmed, S.F.U., Kobayakawa A. 2011b. Corrosion of reinforcing steel in fibre reinforced cementitious composites, Advanced Concrete Technology 9(2), June 2100, 159-167.
Miyazato, S. and Hiraishi, Y. Transport properties and steel corrosion in ductile fiber reinforced cement composites, Proceedings ICF, Turin, Italy, March 2005.
Paul SC, Theunissen AI, van Zijl GPAG 2013a. Chloride induced corrosion in cracked reinforced strain hardening cement-based composites (R/SHCC), In: Proceedings of SCMT3, Kyoto August 2013.
Paul SC, van Zijl GPAG 2013b. Strain hardening cement based composite (SHCC) with fine and coarse sand under tensile load and chloride attack, In: Proceedings of the 8th Int. Conf. on Fracture of concrete and concrete structures (FramCoS-8).
Sahmaran M, Li M, Li VC 2007. Transport properties of engineered cementitious composites under chloride exposure, ACI Materials Journal Nov/Dec 2007, 604-611.
Van Zijl GPAG 2011. Crack distribution characterisation, towards a framework for durability design of Strain-hardening Cement-based Composites (SHCC), Proceedings PRO 81, International RILEM workshop on Strain Hardening Cementitious Composites (SHCC2-Rio), 12-14 Dec 2011, Rio, Brazil, pp. 149-156.
Van Zijl GPAG, Wittmann, FH, Oh BH, Kabele P, Toledo Filho RD, Fairbairn EMR, Slowik V, Ogawa A, Hoshiro H, Mechtcherine V, Altmann F, Lepech MD 2012. Durability of strain-hardening cement-based composites (SHCC), Materials and Structures: Volume 45, Issue 10 (2012): 1447-1463.
Van Zijl GPAG Wittmann FH (eds.) 2011. *Durability of Strain-Hardening Fibre-Reinforced Cement-Based composites (SHCC)*, State-of-the-art report, Rilem TC 208 HFC, SC 2, Springer Publishers, ISBN-13: 978-94-007-0337-7
Wittmann FH, Wang P, Zhang P, Zhao Tie-Jun, Betzung F 2011. Capillary absorption and chloride penetration in neat and water repellent SHCC under imposed strain, 2nd International Conference on Strain Hardening Cementitious Composites, Dec 2011, Rio de Janeiro, pp. 165-172.